**Original Article**

# A Histological Study to Evaluate the Efficacy of the Antidepressant Fluoxetine Versus the Anti-inflammatory Sulfasalazine in Experimentally Induced Colitis in Adult Male Albino Rats

***Azza S. Soliman, Dalia F. Kallini, Rania A. Salah El Din, Haidy F. Abdel Hamid, Sherif A. Kamar and Shimaa M. Mohammed***

*Department of Anatomy, Faculty of Medicine, Ain Shams University, Egypt*

## ABSTRACT

**Background:** The growing prevalence of the inflammatory bowel diseases in Arab community increases both economic and health care burden. Thus, better and more affordable treatment cure is greatly needed.
**Aim of the Work: T**he goal of work was to study the histological effect of the antidepressant drug (fluoxetine) versus the traditional anti-inflammatory drug (sulfasalazine) on induced colitis in adult male albino rats.
**Material and Methods:** Twenty-four adult male albino rats were randomly divided into four groups, each containing six rats.: group (A) which served as the control group; group (B), in which colitis was induced by intra-rectal administration of 1 ml of 2% acetic acid daily for 3 consecutive days then left without any treatment for 14 days; group (C), in which the rats received sulfasalazine for 14 days after induction of colitis as in group B; and group (D) in which the rats received fluoxetine 14 days after induction of colitis. Both drugs in group (C) and (D) were dissolved in distilled water and administered by oral gavage once daily. At the end of the experiment, distal colon (10 cm proximal to the anus) was removed and processed for light microscopic examination using H & E, combined alcian blue – PAS and Mallory's trichrome stains. Toluidine blue stain was used for semi-thin sections. Computer image analysis and statistical study were also performed for the number of goblet cells and area percent of collagen fibers content.
**Results:** Colitis induction showed mucosal injury. There was loss of surface epithelium and disruption of crypt architecture. The muscularis mucosae showed vacuolations. Moreover, there were dilated blood vessels in submucosa. Administration of fluoxetine improved the colonic structure especially the surface epithelium while sulfasalazine was by far less efficient in improving induced colitis.
**Conclusion:** Fluoxetine improved the colonic structure and proved to be more effective management of experimentally induced colitis with less adverse effects than the conventional management by sulfasalazine.

**Received:** 10 August 2017, **Accepted:** 17 September 2017

**Key Words:** Fluoxetine; induced colitis; sulfasalazine.

**Corresponding Author:** Shimaa Magdy Mohammed Mahmoud, Department of Anatomy, Faculty of Medicine, Ain Shams University, Egypt, **Tel.:** +20 10002 72124, **E-mail:** Shimaa_mm13@yahoo.com

**The Egyptian Journal of Anatomy, ISSN:** 0013-2446, Vol. 42 No. 1

## INTRODUCTION

Inflammatory bowel disease (IBD), such as Crohn's disease (CD) and ulcerative colitis (UC) are severe chronic inflammatory disorders of the gastrointestinal tract. There is limited information about the IBD in Arab community. The growing prevalence of this disease increases both economic and health care burden. Thus, better and more affordable treatment and eventually a cure is greatly needed ***(Guemei et al., 2008 and Low et al., 2013)***.

IBD adversely affects the quality of life and necessitates longterm dependence on effective drugs. Mesalazine, sulfasalazine and other 5-aminosalicylic acid (ASA) derivatives are considered currently drugs of choice for the management of most cases. Although these drugs are effective, the risk of their adverse effects is

 *DOI:10.21608/EJANA.2022.249443*

high, especially considering the chronic and relapsing nature of this condition. Therefore, the search for new safer therapies continues ***(Abdel-Aziz et al., 2013)***.

Sulfasalazine (SSZ) consists of one molecule of 5-aminosalicylic acid (5-ASA, mesalamine) coupled by an azo bond to one molecule of sulfapyridine. The azo bond allows uncoupling of the two constituent compounds in the lumen of the colon by the action of bacterial azo reductase enzymes resulting in topical delivery of the compounds. It has been shown that the 5-ASA moiety of SSZ is the therapeutically active component in IBD and that the sulfapyridine moiety is inactive and causes most of the allergic and intolerant effects of SSZ ***(Vigna, 2014)***.

Fluoxetine (FLX) is a selective serotonin reuptake inhibitor of proven efficacy in major depressive disorders. This antidepressant exhibits higher safety and fewer side effects than other groups of antidepressants ***(Guemei et al., 2008 and Koh et al., 2011)***. There are several reports about the analgesic and anti-inflammatory effects of antidepressant drugs; for instance, anti-inflammatory activity of FLX is studied on the carrageenan-induced paw inflammation in the rat ***(Minaiyan et al., 2014)***. FLX is characterized as a lipophilic weak base, which when administered orally experiences a direct contact with epithelial cells in the intestine. In these epithelial cells, it induces an increase in serotonin (5-HT) levels by blocking L-monoamine oxidase and serotonin reuptake transporters ***(Stopper et al., 2014)***.

Acetic acid (AA)-induced colitis is a reproducible and simple model, sharing many characteristics with human colitis ***(Wang et al., 2013)***. Hence, the aim of this study was to illustrate the modulating effects of fluoxetine versus sulfasalazine on the structure of the colon after colitis induction by acetic acid.

## MATERIAL AND METHODS

Twenty-four adult male albino rats weighing (200-250 g.) were used throughout this work. They were housed in suitable environment, in conventional wire-mesh cages, in the Bilharzial research center at Faculty of Medicine Ain-shams University. The plan of the study was done according to guide lines of the CARE (Committee of Animal Research Ethics) of Faculty of Medicine Ain-Shams University. The rats were randomly divided into four groups:

**Group A:** The untreated control group consisted of six rats, which received 1ml distilled water per rectum daily for three consecutive days ***(Hamam et al., 2014)***.

**Group B:** Acetic acid-induced colitis (AAIC) group consisted of six rats, in which colitis was induced by intrarectal administration of 1 ml of 2% acetic acid daily for 3 consecutive days then left without any treatment for 14 days ***(Soliman et al., 2010)***.

**Group C:** AAIC sulfasalazine-treated (SSZ) group in which six rats received sulfasalazine in a dose of 360 mg/kg BW for 14 days after induction of colitis ***(Prakash et al., 2008)***.

**Group D:** AAIC fluoxetine-treated (FLX) group in which six rats received fluoxetine in a dose of 20mg/kg BW for 14 days after induction of colitis ***(Branco-de-Almeida et al., 2012)***.

Both drugs in group C and D were dissolved in distilled water and administered by oral gavage once daily throughout the experimental period (14 days).

### *Induction of experimental colitis in rats*

Rats were kept in a fasting state overnight with access to water ad libitum before the induction of colitis. Rats were anaesthetized by ether inhalation before acetic acid administration. They were subjected to colitis induction by rectal injection of 1 ml of 2% acetic acid in distilled water, once daily for three consecutive days. Acetic acid was infused slowly into the lumen of the colon via an infantile Ryle tube fitted onto 1 ml syringe. The tube was inserted into distal colon 8 cm proximal to the anus. Then the rats were maintained in the trendelenberg position for 30 seconds to allow adequate contact of acetic acid with the mucosal surface ***(Soliman et al., 2010 and Hamam et al., 2014)***.

At the end of the experiment, distal colon (10 cm proximal from the anus) was removed and split longitudinally with scissor. Then, it washed thoroughly with saline and each specimen was divided into two halves. One half was processed for applying the paraffin technique, and the other half was prepared for semithin sections.

### *Light microscopic study*

Formalin (10%) fixed colon slices were processed to form paraffin blocks. Serial sections 5µm in thickness were prepared. The sections were subjected to haematoxylin and eosin stain (H&E),

combined alcian blue-PAS stain and Mallory's trichrome stain. The other half of colon was fixed in 3% phosphate buffered glutaraldehyde and small pieces (1×1mm³) were processed to epon blocks. Sections were stained with toluidine blue ***(Bancroft and Gamble, 2013)***. All sections were examined by light microscope.

### *Computer image analysis*

The TS View image analysis software in the Anatomy Department, Faculty of Medicine, Ain Shams University, was employed. Pixels were calibrated for actual measurements in micrometer. Six randomly chosen fields in six sections obtained from six different animals from the same group were used for measuring each of the following:

- Mean number of goblet cells.
- Mean area percentage of collagen fibers content in colonic wall.

The measurements were taken at high-power fields of magnification (x400) for mean number of goblet cells and at (x100) for the mean area % of collagen fibers.

### *Statistical analysis*

Statistical measures were done using the statistical package for social studies (SPSS – Version 13.0). One way analysis of variance (ANOVA) was employed to compare means between groups. Bonferroni Post hoc test was used to detect significance between every two individual groups.

The significance of the data was determined by the probability (*P- value*). $P > 0.05$ was considered insignificant, $P < 0.05$ was considered significant and $P < 0.01$ was considered highly significant. Data were represented in tables and column charts.

## RESULTS

### *Light microscopic results*

### *Group A (control group)*

The examination of haematoxylin and eosin sections of this group showed a normal colon architecture as its wall was formed of mucosa, submucosa, muscularis externa and serosa. The surface epithelium was intact and the mucosa was formed of closely packed simple tubular glands (crypts of Lieberkühn) that extend in the lamina propria till the muscularis mucosae and open into surface epithelium (Figure 1).

Crypts were lined by colonocytes (absorptive columnar cells with basal nucleus, acidophilic cytoplasm and apical brush border) and goblet cells (mucin-secreting cells with clear cytoplasm and basal compressed nuclei). The lamina propria was seen consisted of the stromal elements investing the crypts and containing eosinophils (Figure 2).

Semi-thin sections stained with toluidine blue showed goblet cells containing darkly -stained mucin and neighboring tall columnar colonocytes having basal oval vesicular nuclei with prominent nucleoli resting on a thin basement membrane. At the apex of each cell present a homogeneous layer called the brush border. Mitotic figures were more evident towards crypt base. In the lamina propria capillaries lined by endothelial cells were observed (Figure 3).

By combined alcian blue-PAS stain, most of goblet cells and the mucus inside the lumina of the crypts showed positive reaction (Figure 4).

Mallory's trichrome stained sections showed that the submucosa was composed of loose connective tissue with minimal amount of fine blue collagen fibers (Figure 5). Arterioles, venules and lymphatics were also seen throughout the submucosa. Muscularis externa was formed of a relatively thick inner circular layer and a thinner coat of outer longitudinal layer (Figure 1).

### *Group (B) (AAIC group)*

Examination of haematoxylin and eosin stained sections showed shedding of the surface epithelium, dilatation of some crypts with cellular debris in the lumen while other crypts showed distortion and branching (Figure 6).

The mucosa showed also crowded crypts within the lamina propria. Most of the crypts were depleted from goblet cells (Figure 7). The lumina of some crypts were obliterated and the muscularis mucosae showed vacuolations (Figure 8). The submucosa showed cellular infiltration and irregularly dilated blood vessels (Figure 9). The muscularis externa showed apparent thickening (Figure 6).

Semi-thin sections of this group showed partial loss of the surface epithelium. Some crypts were lined by apparently normal columnar cells with basally vesicular nuclei and goblet cells (Figure 10). In other sections, the nuclei of the cells lining the crypts showed pleomorphism as they were different in sizes and shapes with irregular contours (Figure 11).

Combined alcian blue-PAS stained sections of this group showed positive reaction for goblet cells and for mucus inside some crypts, while other crypts showed weak reaction being depleted from goblet cells (Figure 12).

Mallory's trichrome stained sections showed apparent increase content of collagen fibers in the submucosa and serosa (Figure 13).

### *Group (C) (SSZ group)*

Examination of haematoxylin and eosin stained sections showed relative restoration of surface epithelium in some areas while there was discontinuity in other areas. Restoration of crypt architecture was also observed with some branched and bifurcated crypts (Figure 14). The mucosa showed also some dilated crypts with flattened epithelial lining. Other crypts were lined by apparently normal columnar cells and numerous goblet cells (Figure 15).There were dilated blood vessels, inflammatory cell infiltrate and arterioles with vacuolations in their walls in the submucosa. Gaping between muscle fibers of muscularis externa was also seen (Figure 16).

In semi-thin sections, the crypts were lined by apparently normal colonocytes having basal vesicular nuclei and goblet cells (Figure 17). Combined alcian blue-PAS sections showed strong positive reaction and restoration of goblet cells (Figure 18). Mallory's trichrome stained sections showed dense collagen fibers in the submucosa surrounded dilated congested blood vessels (Figure 19).

### *Group (D) (FLX group)*

Examination of haematoxylin and eosin stained sections showed restoration of the surface epithelium and the normal architecture of the mucosa (Figure 20). Most of the surface epithelium appeared with its characteristic brush border and the crypts showed restoration of goblet cells (Figure 21).

There were apparently normal blood vessels in the submucosa (Figure 22). Muscularis externa showed apparently normal arrangement of muscle fibers with increased cells of myenteric plexus extending between the muscle fibers (Figure 23).

Semi-thin sections showed apparently normal colonocytes with regular brush border. Few of them had abnormaly shaped nuclei (Figure 24).

Crypts were seen apparently normal and were lined by goblet cells with its characteristic apical mucin granules and columnar cells with basal vesicular nuclei (Figure 25).

Combined alcian blue – PAS sections showed moderate positive reaction of goblet cells (Figure 26).

Mallory's trichrome stained sections showed regular collagen fibers in the submucosa and serosa (Figure 27).

### *Results of image analysis and statistical results*

Mean number of mucin containing goblet cells (GCs):

There was a significant decrease in the mean number of goblet cells in group (B) compared to group (A) with *p-value* 0.04012 while in the treated groups there was a significant increase in group C (SSZ group) in comparison with group (A) with *p-value* 0.00127 and there was a non-significant difference between group D (FLX group) and group (A) with p-value 0.8762 as seen in (Table 1, Chart 1).

Compared with group B, there was significant increase in the mean number of goblet cells in group C with *p-value* 0.000145225, while there was a non-significant difference between group D and group B with *p-value* 0.18077997 as seen in (Table 2, Chart 2).

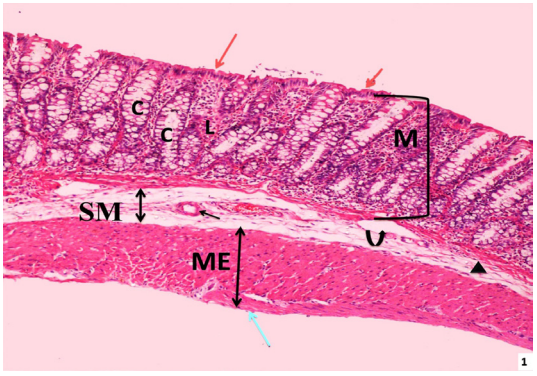


**Fig. 1:** A photomicrograph of a section in the colon of an adult male albino rat of group A (control group) showing the different colon layers: mucosa (M), submucosa (SM), muscularis externa (ME) and serosa (blue arrow). Note the crypts (C) in the mucosa span the lamina propria (L) till muscularis mucosae (arrow head) and arranged in parallel, like a row of test tubes in a rack. Notice the arteriole (black arrow) and lymph vessel (curved arrow) in the submucosa. (Hx&E x 100)

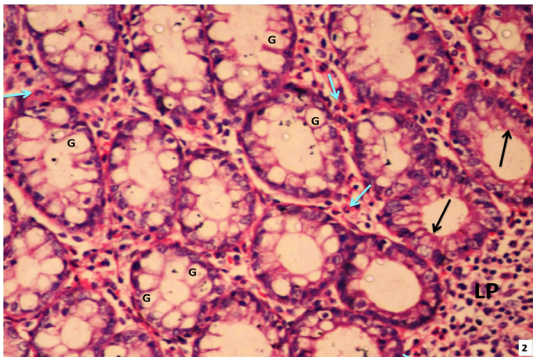


**Fig. 2:** A photomicrograph of a cross section in the colon of an adult male albino rat of group (A), showing columnar colonocytes with basal nucleus, acidophilic cytoplasm and apical brush border (black arrow). Numerous goblet cells (G) with clear cytoplasm and basal compressed nuclei are seen. Notice some eosinophils (blue arrow) in lamina propria ( LP). (Hx&E x 400)

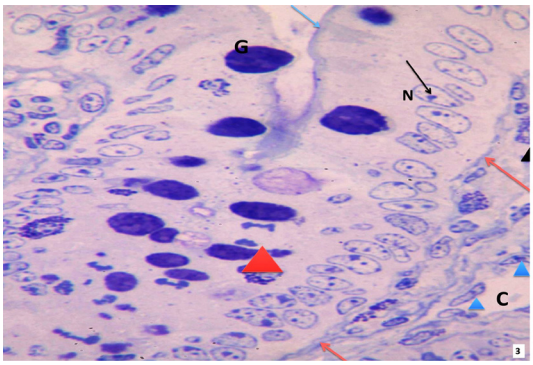


**Fig. 3:** A photomicrograph of a semi-thin section in the colon of an adult male albino rat of group (A), showing darkly -stained mucin of the goblet cells (G). The tall columnar colonocytes with their basal oval nucleus (N) and prominent nucleolus (black arrow) are seen resting on thin basement membrane (red arrows) with their brush border (blue arrow). Note also the presence of mitotic figure (red arrow head) and a capillary (C) lined by endothelial cells (blue arrow head) in the lamina propria. (Toluidine blue x1000)

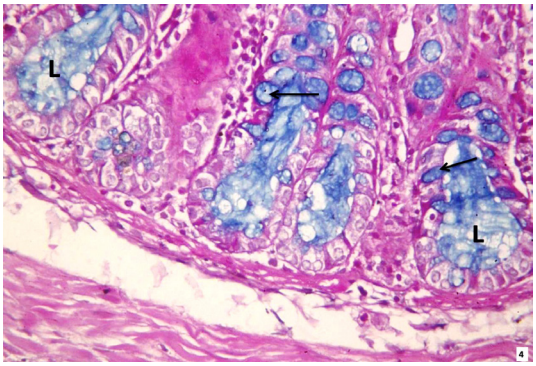


**Fig. 4:** A photomicrograph of a section in the colon of an adult male albino rat of group (A), showing a positive reaction of alcian blue – PAS staining for the goblet cells (arrows) and the mucus inside the lumina of the crypts (L). (Alcian blue – PAS x 400)

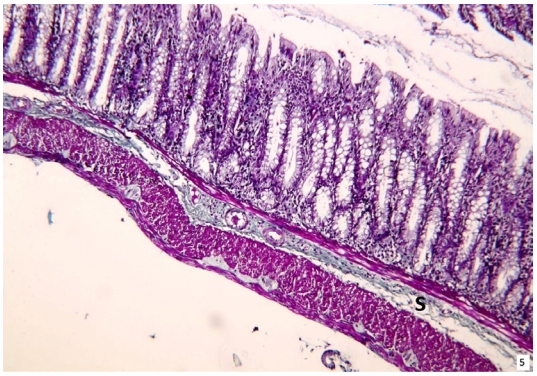


**Fig. 5:** A photomicrograph of a section in the colon of an adult male albino rat of group (A), showing fine blue collagen fibers in the submucosa (S). (Mallory's trichrome x 100)

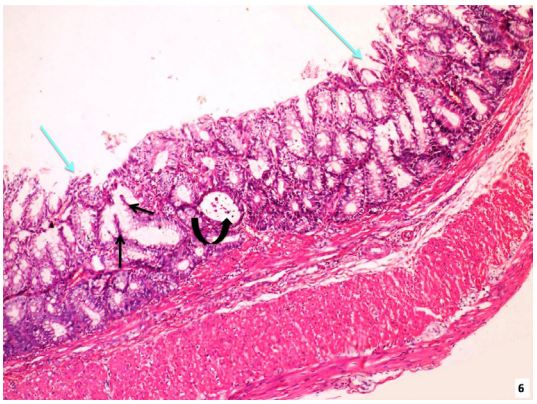

**Fig. 6:** A photomicrograph of a section in the colon of an adult male albino rat of group (B), showing shedding of the surface epithelium (blue arrows), dilatation of a crypt with cellular debris in the lumen (curved black arrow) while other crypts showed distortion and branching (black arrows). Note an apparent thickening of muscularis externa (ME). (Hx&E x 100)

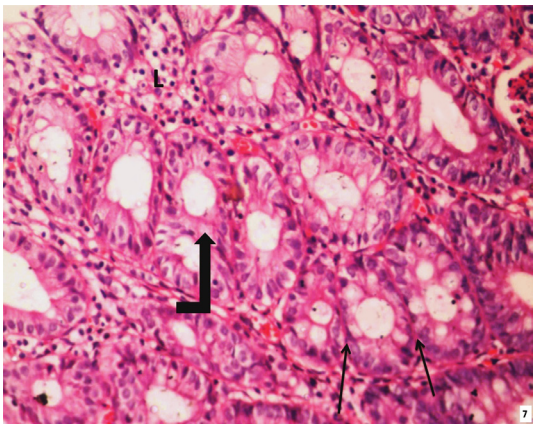


**Fig. 7:** A photomicrograph of a cross section in the colon of an adult male albino rat of group (B), showing crowded crypts (arrows) in the lamina propria (L). Note the presence of branched crypt (curved arrow). (Hx&E x 400)

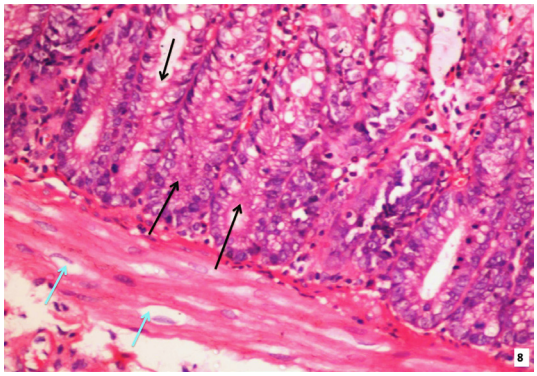

**Fig. 8:** A photomicrograph of a section in the colon of an adult male albino rat of group (B), showing obliterated lumina of some crypts (black arrows) and vacuolations in the muscularis mucosae (blue arrows). (Hx&E x 400)

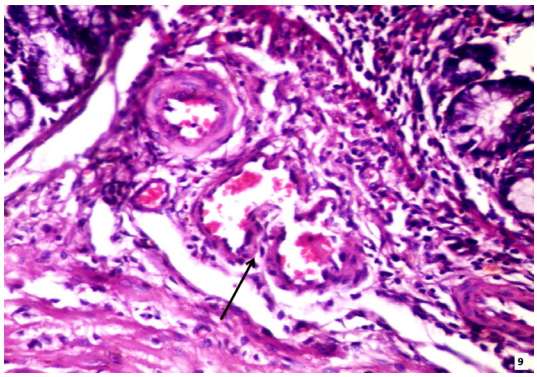

**Fig. 9:** A photomicrograph of a section in the colon of an adult male albino rat of group (B), showing irregular dilatation in submucosal blood vessel surrounded by cellular infiltration (arrow). (Hx&E x 400)

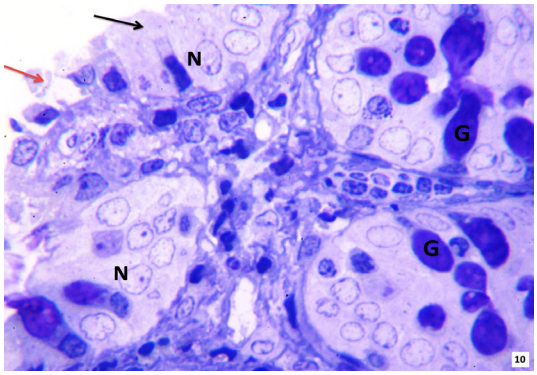


**Fig. 10:** A photomicrograph of a semi-thin section in the colon of an adult male albino rat of group (B) showing the surface epithelium (black arrow) with partial loss (red arrow). Note some crypts are lined by apparently normal goblet cells (G) and columnar cells with their basal nuclei (N) having prominent nucleoli. (Toluidine blue x1000)

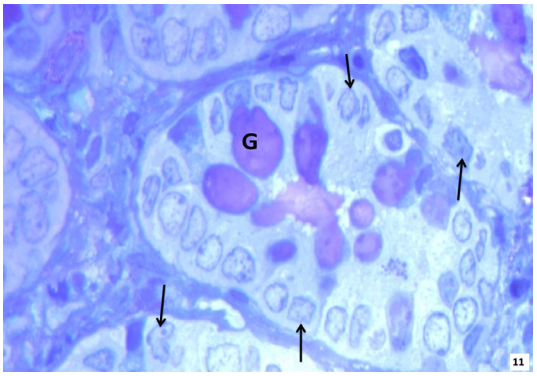


**Fig. 11:** A photomicrograph of a semi-thin section in the colon of an adult male albino rat of group (B) showing a pleomorphism of the nuclei in the cell lining the crypts (arrows).G = goblet cell (Toluidine blue x 1000)

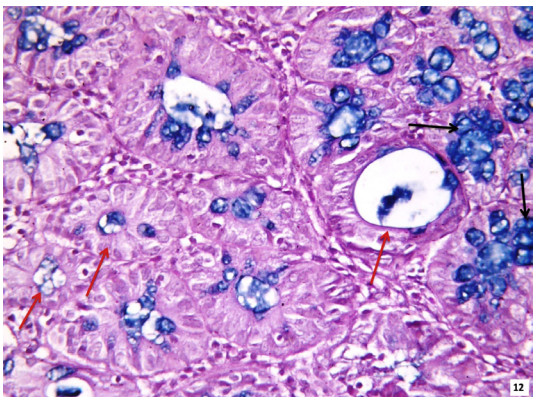

**Fig. 12:** A photomicrograph of a section in the colon of an adult male albino rat of group (B) showing positive reaction of alcian blue – PAS staining for the goblet cells in some crypts (black arrows) while other crypts showing weak reaction (red arrow). (Alcian blue – PAS x 400)

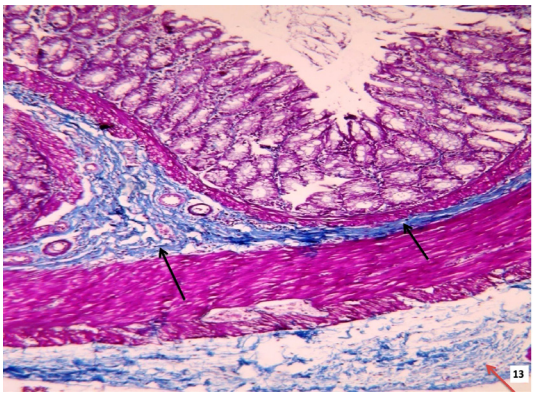

**Fig. 13:** A photomicrograph of a section in the colon of an adult male albino rat of group (B) showing increased collagen fibers in the submucosa (black arrows) and serosa (red arrow). (Mallory's trichrome x 100)

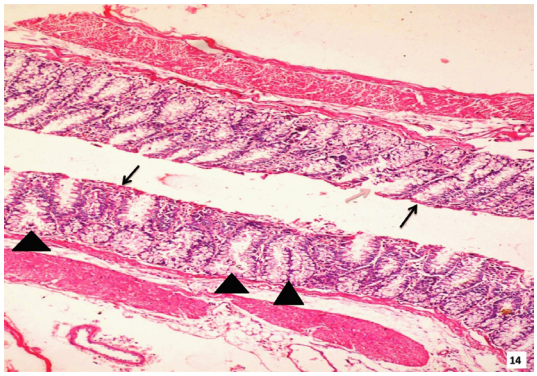

**Fig. 14:** A photomicrograph of a section in the colon of an adult male albino rat of group (C), showing restored surface epithelium (black arrows) with discontinuity in some areas (red arrow) and apparently normal crypt architecture with some branched and bifurcated crypts (arrow head). (Hx&E x 100)

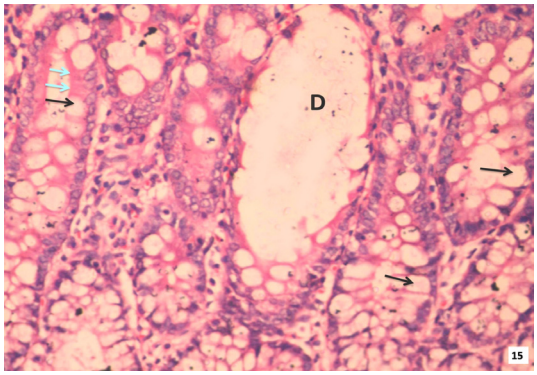


**Fig. 15:** A photomicrograph of a section in the colon of an adult male albino rat of group (C), showing a dilated crypt with flattened epithelial lining (D). Note other crypts are lined by apparently normal columnar cells (blue arrows) and numerous goblet cells (black arrows). (Hx&E x 400)

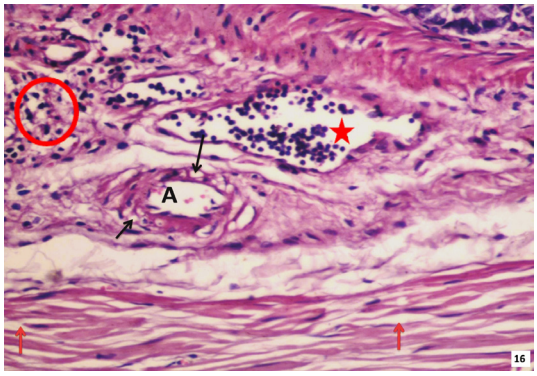


**Fig. 16:** A photomicrograph of a section in the colon of an adult male albino rat of group (C), showing in the submucosa, a dilated blood vessel (star) with inflammatory cell infiltrate (circle) and an arteriole (A) with vacuolations in its wall (black arrows). Note the presence of gaps between muscle fibers of muscularis externa (red arrows). (Hx&E x 400)

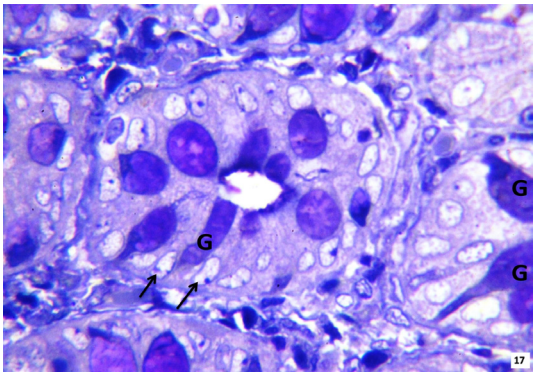


**Fig. 17:** A photomicrograph of a semi-thin section in the colon of an adult male albino rat of group (C), showing the crypts are lined by apparently normal colonocytes having basal vesicular nuclei (arrows) and numerous goblet cells (G). (Toluidine blue x1000)

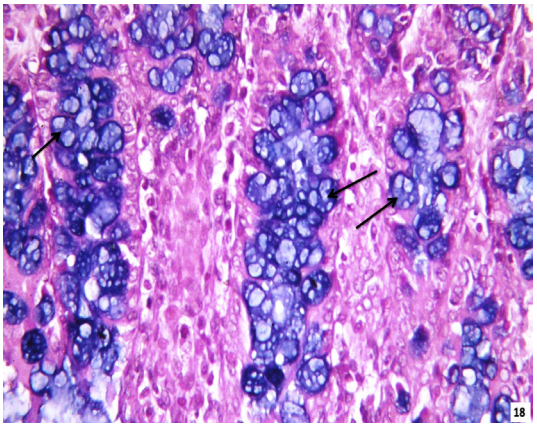

**Fig. 18:** A photomicrograph of a section in the colon of an adult male albino rat of group (C), showing strong positive reaction of Alcian blue – PAS staining for the goblet cells (arrows). (Alcian blue – PAS x 400)

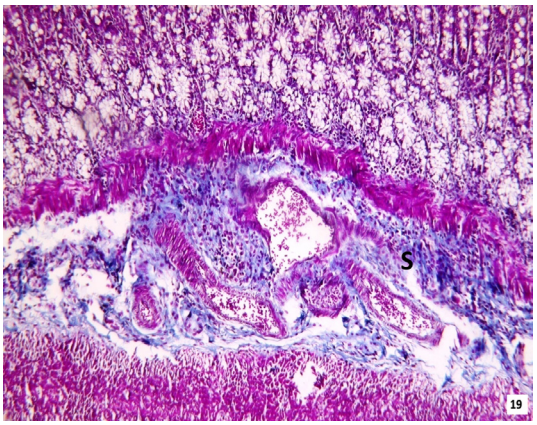


**Fig. 19:** A photomicrograph of a section in the colon of an adult male albino rat of group (C), showing dense collagen fibers surrounding dilated congested blood vessels in the submucosa (S). (Mallory's trichrome x 100)

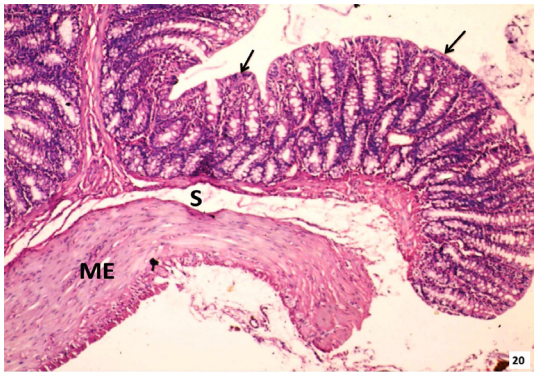


**Fig. 20:** A photomicrograph of a section in the colon of an adult male albino rat of group (D), showing restoration of the surface epithelium (arrows) and the normal architecture of the mucosa. S = submucosa, ME = muscularis externa (Hx&E x 100)

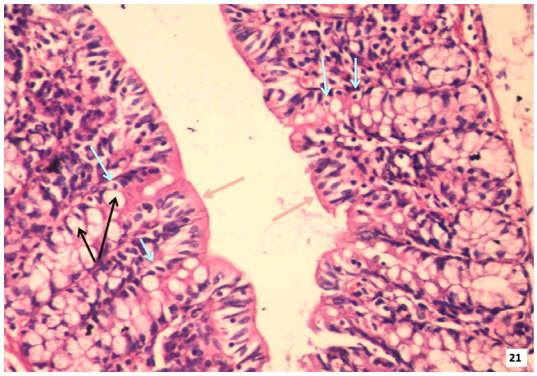


**Fig. 21:** A photomicrograph of a section in the colon of an adult male albino rat of group (D), showing surface epithelium with its characteristic brush border (red arrows) and the crypts are lined by numerous goblet cells (black arrows). (Hx&E x 400)

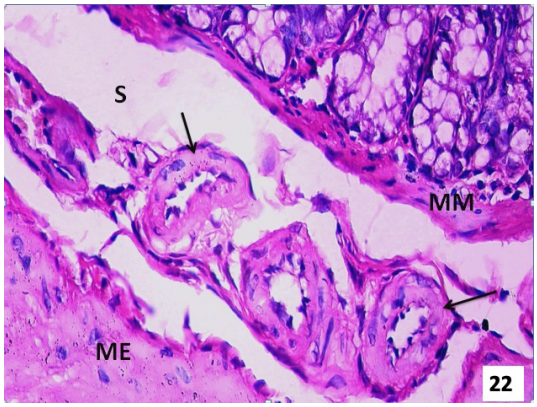


**Fig. 22:** A photomicrograph of a section in the colon of an adult male albino rat of group (D), showing apparently normal arterioles (arrows) in the submucosa (S). MM = Muscularis mucosae, ME = Muscularis externa. (Hx&E x 400)

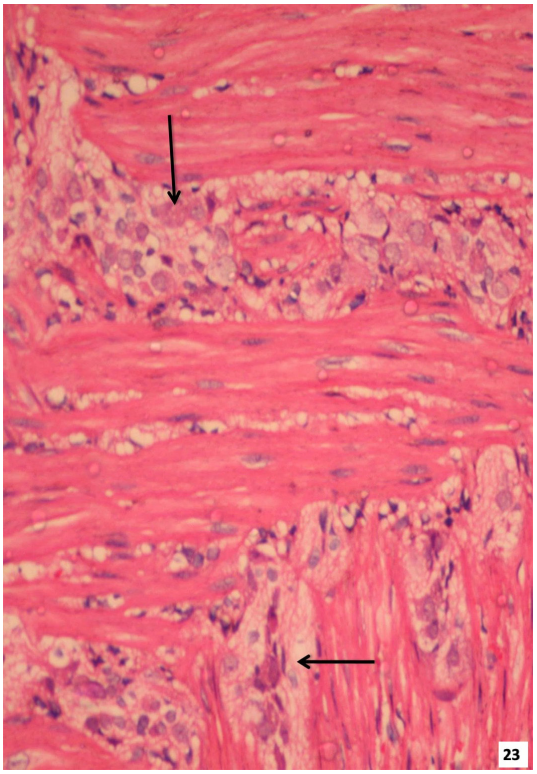


**Fig. 23:** A photomicrograph of a section in the colon of an adult male albino rat of group (D), showing an apparently normal arrangement of muscle fibers in the muscularis externa. Note the increased cells of myenteric plexus extending between the muscle fibers (arrows). (Hx&E x 400)

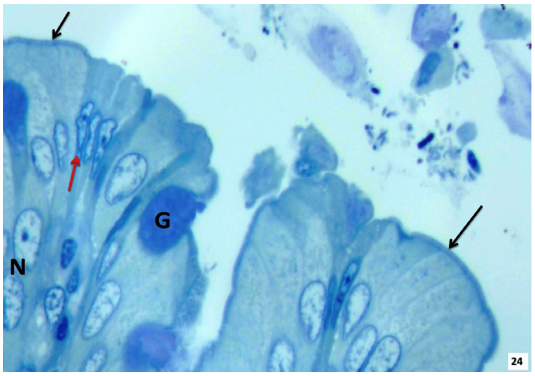


**Fig. 24:** A photomicrograph of a semi-thin section in the colon of an adult male albino rat of group (D), showing apparently normal colonocytes with basal vesicular nucleus (N) and regular brush border (black arrows). Note that few of the colonocytes have abnormally shaped nuclei (red arrow). (Toluidine blue x1000)

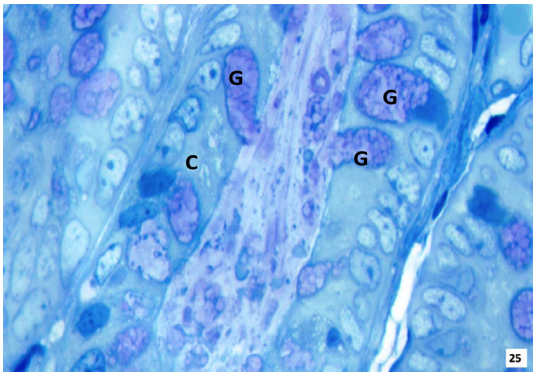


**Fig. 25:** A photomicrograph of a semi-thin section in the colon of an adult male albino rat of group (D), showing apparently normal crypts lined by goblet cells with its characteristic apical mucin granules (G) and columnar cells with basal vesicular nuclei (C). (Toluidine blue x1000)

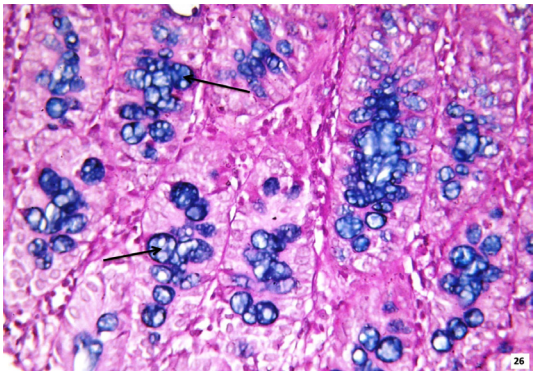


**Fig. 26:** A photomicrograph of a section in the colon of an adult male albino rat of group (D), showing moderate positive reaction and restoration of goblet cells (arrows). (Alcian blue – PAS x 400)

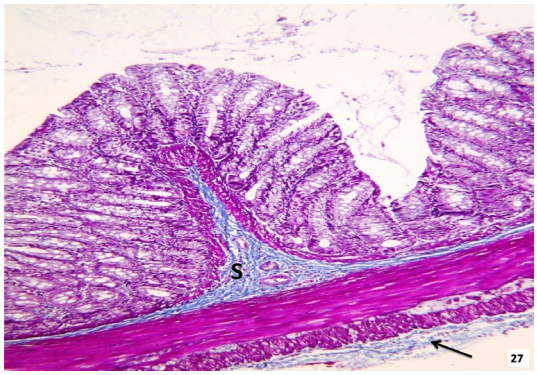


**Fig. 27:** A photomicrograph of a section in the colon of an adult male albino rat of group (D), showing collagen fibers in the submucosa (S) and serosa (arrow). (Mallory's Trichrome x 100)

**Table 1:** Means ± SD of number of GCs in all studied groups

| Group | A | B | C | D |
|---|---|---|---|---|
| Mean number of GCs ± SD | 51.66667 ± 3.386247 | 46 ± 4.816638 | 61 ± 3.898718 | 52.33333 ± 9.647107 |
| *P-value* (compared with A) | | 0.0401257* | 0.001279717^ | 0.876282324 |
| *P-value* (compared with B) | | | 0.000145225^ | 0.18077997 |

*, Significant decrease.
^, Significant increase.

**Table 2:** Mean area % of CFs in the colon wall in all studied groups

| Group | A | B | C | D |
|---|---|---|---|---|
| Mean % of CFs content | 3.31% | 11.59% | 8.28% | 6.63% |
| *P-value* (compared with A) | | 0.0000000001^ | 0.0000000004^ | 0.0000000037^ |
| *P-value* (compared with B) | | | 0.0000018787* | 0.000000022* |

^, High significant increase.
*, High significant decrease.

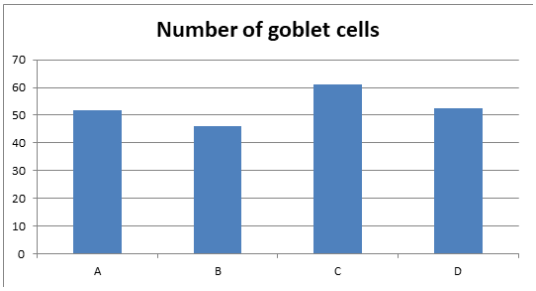


**Chart 1:** Means of number of GCs of all studied groups

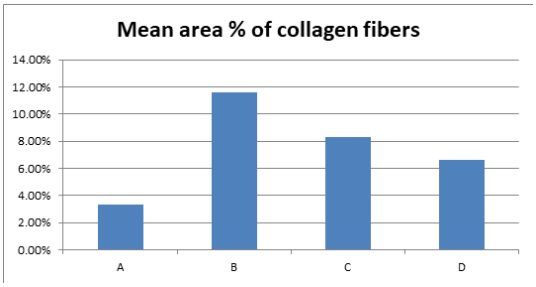


**Chart 2:** Mean area % of CFs in the colon wall in all studied groups

## DISCUSSION

Inflammation is a defensive process that a living body initiates against local tissue damage or the presence of inflammatory stimulants. However, when this process of inflammation is not controlled properly via competent negative feedback, a chronic low-grade inflammatory state could result ***(Medzhitov, 2008)***.

Colitis can occur from viral or bacterial infections, ischemic insult, or autoimmune disorders; most notably UC and CD. The complex interactions between the environment, genetics, and epithelial barrier dysfunction in IBD and animal models of colitis have been essential in advancing the knowledge of this disease ***(Whittem et al., 2010)***.

The chronic and intermittent nature of IBD and inability of the current drugs to sustain long-term remission made a continuous need to testify new drugs aiming to minimize the morbidity and to improve the quality of patient's life ***(Galil et al., 2015)***.

The present study aimed to show the colonic tissue damage induced by intrarectal acetic acid application, and to demonstrate the probable recovery in the colon tissue with flouxetine therapy versus sulfasalazine and the possible underlying mechanism. Mehrabani et al. (2011) stated that various chemical compounds have been applied for induction of experimental colitis in animal models and that acetic acid induced colitis models were identical to human UC in terms of histopathological changes. Moreover, Vemu et al. (2016) mentioned that in induced models of colitis, dextran sodium sulfate and 2, 4, 6-trinitrobenzene sulfonic acids were the commonly used models in mice whereas acetic acid and indomethacin models were commonly used in rats. Tanideh et al., (2014) added that intrarectal acetic acid injection was an easy, repeatable, and cost-effective method for experimental colitis on small laboratory animals. Minaiyan et al., (2014) explained the mechanism of induction of UC by acetic acid. The authors mentioned that the protonated form of the acid liberates protons within the intracellular space and causes a massive intracellular acidification resulting in massive epithelial damage. The inflammatory response initiated by acetic acid includes activation of cyclooxygenase and lipooxygenase pathways.

Wada-Hiraike et al., (2006) stated that estrogen has a protective effect on the colonic mucosa and reported that relative absence of estrogen in postmenopausal women as well as in men were associated with increased levels of reactive oxygen species (ROS) as well as with the risk of several diseases such as UC. Male albino rats were used in the present study to avoid the protective effect of estrogen.

In the current study, areas of mucosal surface loss were observed in-group B (AAIC). Some crypts were dilated and distorted, while others were branched and crowded. Other crypts appeared intact and were lined with absorptive and goblet cells. The branching and restoration of normal crypts were most likely signs of regeneration. Soliman et al., (2010) suggested that the presence of signs of regeneration, as nearly regular crypts lined by columnar and goblet cells, might be acceptable as the rats were sacrificed after 14 days of UC induction, which allowed such regeneration. Nevertheless, this period failed to induce complete improvement of the colonic architecture, as the inflammatory process together with ongoing attempts of regeneration resulted in progressive crypt distortion.

The nuclei of some colonocytes in the semithin sections obtained from group B showed pleomorphism and irregular contour. These results may be either dysplastic, as described by Odze (2006) or reactive as reported by Cheng & Bostwick (2011).

In the current work the morphometric study revealed that the number of goblet cells showed significant decrease in group B compared to group A. This finding was in agreement with Mahmoud et al., (2015) who reported that the colonic mucosa of the colitis group showed loss of goblet cells, indicated by the reduction in the number of alcian blue-positive cells in the mucosa of the colon. Imaeda et al., (2011) explained that reduction in the number of alcian blue-positive cells had been previously related to alterations in the normal pattern of maturation of mucin in goblet cells. This decreased the protective effect of mucus as an active barrier leading to accumulation of ROS and development of the inflammation process causing tissue damage.

There were vacuolations and increased intercellular spaces in the muscularis mucosae in-group (B) in the present work. This finding was in agreement with Mahmoud et al., (2015) who reported that vacuolar degenerative changes were seen inside the muscularis mucosae in the group of acetic acid induced colitis.

Dilated blood vessels in the submucosa of group B were also noticed, in the present study. This was in accordance with Hartmann et al. (2012) who reported vascular dilatation and white blood cells accumulation in an AA induced model of IBD. This was associated with an increased blood flow leading to increased production of oxygen and hence the excessive generation of free radical and reactive oxygen species. Kruschewski et al., (1995) reported also, dilatation of the submucosal veins together with caliber differences in the tunica muscularis and rarefaction of the penetrating blood vessels in the presence of chronic inflammatory bowel disease.

The submucosa showed highly significant increase of the mean area % of collagen fibers in group B compared to control group A in the present work. This was in agreement with the results of Soliman et al., (2010). In that respect, Valatas et al., (2017) explained that extracellular matrix (ECM) production depends on the activation state of ECM-producing myofibroblasts. Activation and proliferation of myofibroblasts by inflammatory and profibrotic mediators was a central event in the process of normal wound healing after acute injury.

In the current work, rats received sulfasalazine at a dose of 360 mg/kg BW for 14 days after induction of colitis (group C) showed beginning of restoration of surface epithelium and crypts architecture with some bifurcated or branched and dilated crypts. Bjerknes & Cheng (2005) reported that the presence of branched crypts could be explained, as it is an important component of mucosal repair after its injury. Moreover, Linares et al., (2011) stated that although SSZ and 5-aminosalicylic acid scavenge ROS, which may account for some of their anti-inflammatory properties, the reaction with ROS may also generate toxic free radicals; hence, the ability of other antioxidants to suppress the toxicity of SSZ in vivo.

The mean number of goblet cells showed significant increase in-group (C) compared to group (A) and group (B). This suggested that SSZ might play stimulatory effect on the GC differentiation and maturation leading to the increase in their numbers and secretions. This can explain the severe positive reaction of Alcian blue-PAS in this group. However, Lam et al., (2002) stated that excessive goblet cell production might be disadvantageous, as it would come at the expense of enterocytes, compromising absorbing capacities.

The mean area % of collagen fibers in group (C) showed highly significant decrease as compared to group (B). Regarding SSZ antifibrotic effects, Oakley et al., (2005) stated that SSZ might protect against fibrosis by accelerating apoptosis in stellate cells. Additionally, Chávez et al., (2012) reported that in an experimental study of carbon tetra-chloride (CCl4) induced liver fibrosis, SSZ showed antifibrotic effects because of its antioxidant ability and its ability to inhibit NFκB nuclear translocation.

The present study revealed gaping between muscle fibers of muscularis externa in-group (C). Talapka et al., (2016) explained that while the rapid and widespread loss of myenteric neurons was a characteristic feature of the onset of acute inflammation, the precise timing of the cellular events in the chronic phase leading to the intestinal stricturing showed early affection of the smooth muscle cells (SMCs) in the muscularis externa (ME) in these processes. Since the excess deposition of extracellular matrix (ECM) in the ME was sustained throughout the experimental period, the SMCs progressively moved away from each other and from the myenteric ganglia, leading eventually to deficient innervation and severe cellular damage.

In the present study, rats received fluoxetine at a dose of 20 mg/kg BW administered for 14

days after induction of colitis (group D) showed significantly accelerated recovery of colonic wall integrity. There was restoration of the surface epithelium with continuous and well-defined brush border and normal architecture of crypts with minimal disturbance in some areas. These findings coincided with the results of Guemei et al., (2008).

Jin et al., (2009) have shown that FLX strongly suppressed proinflammatory markers, such as cyclooxygenase-2 (COX-2) in neuronal cells. In addition, decreased proinflammatory properties in peritoneal macrophages, redirecting them towards anti-inflammatory activity had been reported in Roman et al., (2009) study. Moreover, Hui-Chen et al., (2012) reported that FLX also inhibited lipopolysaccharide -induced release of nitric oxide (NO) and prostaglandin E2 (PGE2) in serum and cyclooxygenase-2 (COX-2).

Regarding the antioxidant effect of FLX, Kolla et al., (2005) found that pretreatment with FLX was associated with increased superoxide dismutase in cultured rat pheochromocytoma cells. Guemei et al., (2008) reported that FLX in doses of 10 and 20 mg/kg increased significantly the reduced glutathione concentration in ulcerative colonic tissue compared with nontreated control rats.

Numerous cells of the myenteric plexus extending between the muscle fibers of the muscularis externa were observed in-group (D). Similarly, Khodanovich et al., (2016) reported that FLX increased neurogenesis in hippocampal dentate gyrus post global transient ischemia.

Morphometric study revealed that there was a non-significant difference between group D (FLX group) and group (A) regarding the number of goblet cells and this indicates that FLX group was the closest to the control group. In addition, FLX showed a significant decrease in mean area % of collagen fibers as compared to group B and this finding suggested that the FLX could have an antifibrotic effect.

In summary, the present study confirms the knowledge about the anti-inflammatory effect of FLX on AAIC in rats. It is not deniable that people with IBD in general practice suffer from depression or anxiety as a reaction to living with this disease and this can exacerbate the clinical course of IBD. Therefore, treatment of depression by an antidepressant drug that has beneficial effect in the course of underlying disease invokes the proverb “kill two birds with one stone” ***(Mikocka-Walus et al., 2007)***.

## CONCLUSION

The present study suggests that fluoxetine may be considered a promising new therapeutic approach to treat IBD, as it has a positive effect in the AAIC treatment, which is somewhat superior to sulfasalazine, and has fewer side effects. Thus, it is advised to be used in combination with other drugs in the treatment of UC. For better understanding of the mechanisms by which fluoxetine modulates host response, further studies must be conducted.

## CONFLICT OF INTERESTS

There are no conflicts of interest.

## REFERENCES

**Abdel-Aziz H., Wadie W., Abdallah D.M., Lentzen G. and Khayyal M. T. (2013).** Novel effects of ectoine, a bacteria-derived natural tetra -hydropyrimidine, in experimental colitis. Phytomedicine; 20(7): 585-91.

**Bancroft J. and Gamble M. (2013).** Bancroft’s theory and practice of Histological techniques. Elsevier (seventh edition): 69-95.

**Bjerknes M. and Cheng H. (2005).** Gastrointestinal Stem Cells. II. Intestinal stem cells. American Journal of Physiology; 289(3): G381-G387.

**Branco-de-Almeida L. S., Franco G. C., Castro M. L. and Dos Santos J.G., et al. (2012).** Fluoxetine inhibits inflammatory response and bone loss in a rat model of ligature-induced periodontitis.J Periodontol.; 83(5): 664-71.

**Chávez E., Castro-Sánchez L., Shibayama M. and Tsutsumi V et al (2012).** Sulfasalazine prevents the increase in TGF-β, COX-2, nuclear NFκB translocation and fibrosis in CCl4-induced liver cirrhosis in the rat. Hum ExpToxicol.; 31(9):913–920.

**Cheng L. and Bostwick D.G. (2011).** Essentials of Anatomic Pathology. 3rd ed. Springer Science and Business Media; 36-37.

**Galil T.A.E., ElGhamrawy T.A. and Sadik A.O.E. (2015).** The Effect of N. Acetylcysteine and Ginger on Acetic Acid Induced Colitis in Adult Male Albino Rat: Histological, Immunohistochemical and Morphometric Study. J.CytolHistol S3:021.

**Guemei A. A., El Din N. M., Baraka A. M. and El Said I. (2008).** Do desipramine [10, 11-dihydro-5-[3-(methylamino) propyl]-5H-dibenz[b,f]azepine monohydrochloride] and fluoxetine [N-methyl-3-phenyl-3-[4-(trifluoromethyl)phenoxy]-propan-1-amine] ameliorate the extent of colonic damage induced by acetic acid in rats?. J Pharmacol Exp. Ther. ; 327(3): 846-50.

**Hamam, G. G., Raafat, M. H. and Shoukry Y. (2014).** Possible protective effect of dietary extra-virgin olive oil on experimentally induced acute colitis in adult male albino rats: a histological and immunohistochemical study.The Egyptian Journal of Histology; 37: 373-385.

**Hartmann R.M., Morgan M.I., Tieppo J., Fillmann H.S. and Marroni N.P. (2012).** Effect of Boswelliaserrata on antioxidant status in an experimental model of colitis rats induced by acetic acid. Dig Dis Sci.; 57:2038–2044.

**Hui-Chen S., Ching-Ting M., Bu-Chin Y. and Yu-Chieh C., et al. (2012).** Glycogen synthase kinase-3β regulates anti-inflammatory property of fluoxetine, International Immunopharmacology; 14(2): 150-156.

**Imaeda H., Andoh A., Aomatsu T. and Uchiyama K., *et al.* (2011).** Interleukin-33 suppresses Notch ligand expression and prevents goblet cell depletion in dextran sulfate sodium-induced colitis. Int J.Mol Med; 28:573-8.

**Jin Y., Lim C.M., Kim S.W., Park J.Y. and Seo J.S., et al. (2009).** Fluoxetine attenuates kainic acid-induced neuronal cell death in the mouse hippocampus. Brain Res., 1281:108-116

**Khodanovich M.Y., Kisel A.A., Chernysheva G.A. and Smol'yakova V.I., et al. (2016).** Effect of fluoxetine on neurogenesis in hippocampal dentate gyrus after global transient cerebral ischemia in rats. Bulletin of Experimental Biology and Medicine; 161(3):351–54.

**Koh S. J., Kim J. M., Kim I. K. and Kim N., et al. (2011).** Fluoxetine inhibits NF-{kappa} B signaling in intestinal epithelial cells, and ameliorates experimental colitis and colitis-associated colon cancer in mice. Am J PhysiolGastrointest Liver Physiol; 301(1): G9–19.

**Kolla N., Wei Z., Richardson J.S., and Li X.M. (2005).** Amitriptyline and fluoxetine protect PC 12 cells from cell death induced by hydrogen peroxide. J Psychiatry Neurosci 30: 196-201.

**Kruschewski M., Busch C., Dörner A. and Lierse W.(1995).** Angio-architecture of the colon in Crohn disease and ulcerative colitis. Light microscopy and scanning electron microscopy studies with reference to the morphology of the healthy large intestine. Langenbecks Arch Chir.: 380(5):253-9.

**Lam M.M., O'Connor T.P. and Diamond J (2002).** Loads, capacities and safety factors of maltase and the glucose transporter SGLT1 in mouse intestinal brush border. J Physiol 542: 493–500.

**Linares V., Alonso V. and Domingo J. (2011).** Oxidative stress as a mechanism underlying sulfasalazine-induced toxicity. Expert Opin Drug Saf.; 10(2):253–263.

**Low D., Nguyen D. and Mizoguchi E. (2013).** Animal models of ulcerative colitis and their application in drug research. Drug Des DevelTher.; 7: 1341–1357.

**Mahmoud B.L., Shady A. M., Kifafy M. A, El-Seify G. H, Eldamhogy R. A and Omara R. S. (2015).** The effect of royal jelly versus sulfasalazine on acetic acid-induced colitis in adult albino rats. Menoufia Medical Journal; 28: 748-756.

**Medzhitov R. (2008).** Origin and physiological roles of inflammation. Nature; 454:428-35.

**Mehrabani D., Ziaei M., Hosseini S.V. and Ghahramani L., et al. (2011).** The effect of calendula officinalis in therapy of acetic Acid induced ulcerative colitis in dog as an animal model. Iran Red Crescent Med J.; 13:884–890.

**Mikocka-Walus A. A., Turnbull D. A. and Moulding N. T. (2007).** "Controversies surrounding the comorbidity of depression and anxiety in inflammatory bowel disease patients: a literature review," Inflammatory Bowel Diseases; 13 (2):225–234.

**Minaiyan M., Hajhashemi V., Rabbani M., Fattahian E. and Mahzouni P. (2014).** Beneficial Effects of Maprotiline in a Murine Model of Colitis in Normal and Reserpinised Depressed Rats. International Scholarly Research Notices; 359-841.

**Oakley F., Meso M., Iredale J. P., Green K., Marek C. J. and Zhou X., et al. (2005).** Inhibition of inhibitor of kappaB kinases stimulates hepatic stellate cell apoptosis and accelerated recovery from rat liver fibrosis. Gastroenterology 128, 108–12010.

**Odze R. D. (2006).** Pathology of dysplasia and cancer in inflammatory bowel disease. Gastroenterol Clin North Am.; 35:533–552.

**Prakash O. , Medhi B. , Saikia U. N. and Pandhi P. (2008).** Effect of different doses of thalidomide in experimentally induced inflammatory bowel disease in rats. Basic ClinPharmacolToxicol; 103(1): 9-16.

**Roman A., Rogoz Z., Kubera M., Nawrat D. and Nalepa I. (2009).** Concomitant administration of fluoxetine and amantadine modulates the activity of peritoneal macrophages of rats subjected to a forced swimming test. Pharmacol. Rep., 61:1069-1077.

**Soliman N. B. E., Kalleny N. K. and Abd El Samad A. A. (2010).** Effect of Omega-3 versus Omega-6 Fatty Acids on Induced Ulcerative Colitis in Male Albino Rat. Light and Electron Microscopic Study. Egypt. J. Histol.; 33: 620 – 634.

**Stopper H. , Garcia S. B., Waaga-Gasser A. M. and Kannen V. (2014).** Antidepressant fluoxetine and its potential against colon tumors. World J GastrointestOncol; 6(1): 11–21.

**Talapka P., Berkó A., Nagy L. I., Chandrakumar L., Bagyánszki M. and Puskás L. G., et al. (2016).** Structural and molecular features of intestinal strictures in rats with Crohn's-like disease. World Journal of Gastroenterology, 22(22), 5154–5164.

**Tanideh N., Masoumi S., Hosseinzadeh M., Safarpour A. R., Erjaee H., et al. (2014).** Healing Effect of PistaciaAtlantica Fruit Oil Extract in Acetic Acid-Induced Colitis in Rats. Iranian Journal of Medical Sciences. 39.

**Valatas V., Filidou E., Drygiannakis I. and Kolios G. (2017).** Stromal and immune cells in gut fibrosis: the myofibroblast and the scarface. Annals of Gastroenterology, 30(4), 393–404.

**Vemu B., Selvasubramanian S. and Pandiyan V. (2016).** Emu oil offers protection in Crohn's disease model in rats. BMC Complementary and Alternative Medicine, 16, 55.

**Vigna S. R. (2014).** 5-Aminosalicylic Acid Inhibits Acute Clostridium difficileToxin A-Induced Colitis in Rats. International Journal of Inflammation; 2014: 389621.

**Wada-Hiraike O., Warner M. and Gustafsson J.A. (2006).** New developments in oestrogensignalling in colonic epithelium. BiochemSoc Trans; 34 (Pt 6):1114-6.

**Wang Q., Hou Y., Yi D. and Wang L., et al. (2013).**Protective effects of N-acetylcysteine on acetic acid-induced colitis in a porcine model. BMC Gastroenterology; 13: 133.

**Whittem C. G., Williams A. D and Williams C. S. (2010).** Murine Colitis Modeling using Dextran Sulfate Sodium (DSS). Journal of Visualized Experiments:JoVE, (35), 1652.

# دراسة هستولوجية لتقييم فاعلية فلوكستين المضاد للاكتئاب مقابل سلفاسالازين المضاد للالتهاب في التهاب القولون المستحث تجريبياً في الجرذان البيضاء

عزة صلاح الدين سليمان، داليا فوزي قليني، رانيا أحمد صلاح الدين، هايدي فريد عبدالحميد، شريف عادل قمر، شيماء مجدي محمد
قسم التشريح وعلم الأجنة – كلية الطب – جامعة عين شمس

## ملخص البحث

**المقدمة:** تزايد انتشار أمراض الأمعاء الالتهابية في المجتمع العربي يزيد من العبء الاقتصادي والصحي على حد سواء ، وبالتالي هناك حاجة إلى إتاحة علاج أفضل . إن أمراض التهاب الأمعاء تؤثر سلبا على نوعية الحياة وتتطلب الاعتماد على المدى البعيد على الأدوية الفعالة. تعتبر ميسالازين، وسلفاسالازين وغيرها من مشتقات حمض -5أمينوساليسيليك حاليا عقاقير مفضلة لإدارة معظم الحالات، ورغم أن هذه العقاقير فعالة إلا أن خطر آثارها الجانبية مرتفع، خاصة بالنظر إلى طبيعة المرض المزمنة والانتكاس الذي يحدث فيه. ولذلك، يستمر البحث عن علاجات جديدة أكثر أمنا.

**الهدف من العمل:** دراسة القولون نسيجيا لتقييم فاعلية فلوكستين المضاد للاكتئاب مقابل سلفاسالازين المضاد للالتهاب في التهاب القولون المستحث تجريبيا في الجرذان البيضاء.

**الطرق والوسائل:** فى هذا البحث تم استخدام عدد اربعة وعشرون من ذكور الجرذان البيضاء و تم تقسيم الجرذان عشوائيا إلى أربعة مجموعات كل مجموعة تحتوي على عدد ستة من الجرذان كالآتي:

المجموعة الأولي :(المجموعة الضابطة): لم يتم التدخل معهم بأى نوع من العلاجات.

المجموعة الثانية: مجموعة التهاب القولون المستحث والتي تم حقنها بحمض الخليك ( 1ملليلتر بتركيز% 2 )عن طريق فتحة الشرج لثلاثة أيام متتالية ثم تم تركها بدون علاج لمدة 14 يوم.

المجموعة الثالثة: مجموعة العلاج بالسلفاسالازين والتي تلقت عقار السلفاسالازين بجرعة 360 مجم/ كجم من وزن الجسم يوميا لمدة 14 يوم بعد احداث التهاب بالقولون بحمض الخليك.

المجموعة الرابعة: مجموعة العلاج بالفلوكستين والتي تلقت عقار الفلوكستين بجرعة 20 مجم/ كجم من وزن الجسم يوميا لمدة 14 يوم بعد احداث التهاب بالقولون بحمض الخليك.

كلا الدوائين تم إذابتهم في ماء مقطر وإعطائهم عن طريق الفم ، وبعد إتمام التجربة تم التضحية بالحيوانات و أخذ عينات القولون (10 سم من فتحة الشرج ) مع تجهيزها لدراستها و فحصها بالمجهرالضوئى باستخدام صبغه الهيماتوكسلين والايوسين و المالورى ثلاثي الكروم والالشين الازرق مع حمض البريودك شيف.كما استخدمت شرائح شبه رقيقة مصبوغة بصبغة التلويدين الزرقاء. كما استخدم نظام الكمبيوتر المحلل للصور لقياس عدد الخلايا الكأسيه و المساحه المئويه لترسيبات الياف الكولاجين وعمل دراسة إحصائيه .

**النتائج:** أظهر التهاب القولون المستحث في المجموعة الثانية إصابة الطبقة المخاطية للقولون. كان هناك فقدان للسطح وخلل في الشكل المعماري العام للغدد وفجوات في طبقة العضلة المخاطية. وعلاوة على ذلك، كان هناك اتساع في الأوعية الدموية في الطبقة تحت المخاطية . العلاج بالسالفاسالازين كان أقل كفاءة من العلاج بالفلوكستين حيث أدى لنتائج أفضل، فلقد أعاد تركيب الطبقة المخاطية وخاصةً السطح إلى طبيعته بشكل كبير.

**الخلاصة:** كان العلاج بالفلوكستين له تأثير أفضل في تخفيف التهاب القولون المستحث تجريبيا وهو أقل في الآثار السلبية مقارنةً بالسالفاسالازين لذلك نوصي باستخدامه كبديل أو مصاحب لعلاج السالفاسالازين. كما نوصي بعمل المزيد من الدراسات لفهم الآليات التي يعمل بها عقار الفلوكستين.